

This is a self-archived version of an original article. This version may differ from the original in pagination and typographic details.

Author(s): Salama, Eid E.; Youssef, Mohamed F.; Boraie, Ahmed T., A.; Haukka, Matti; Soliman, Saied M.; Barakat, Assem; Sarhan, Ahmed A. M.

Title: Base-Controlled Regiospecific Mono-Benzylation/Allylation and Diallylation of 4-Aryl-5-indolyl-1,2,4-triazole-3-thione : Thio-Aza Allyl Rearrangement

Year: 2023

Version: Published version

Copyright: © 2023 by the authors. Licensee MDPI, Basel, Switzerland

Rights: CC BY 4.0

Rights url: <https://creativecommons.org/licenses/by/4.0/>

Please cite the original version:

Salama, E. E., Youssef, M. F., Boraie, A. T., Haukka, M., Soliman, S. M., Barakat, A., & Sarhan, A. A. M. (2023). Base-Controlled Regiospecific Mono-Benzylation/Allylation and Diallylation of 4-Aryl-5-indolyl-1,2,4-triazole-3-thione : Thio-Aza Allyl Rearrangement. *Crystals*, 13(7), Article 992. <https://doi.org/10.3390/cryst13070992>

Article

Base-Controlled Regiospecific Mono-Benzoylation/Allylation and Diallylation of 4-Aryl-5-indolyl-1,2,4-triazole-3-thione: Thio-Aza Allyl Rearrangement

Eid E. Salama ^{1,*}, Mohamed F. Youssef ¹ , Ahmed T. A. Boraie ¹, Matti Haukka ² , Saied M. Soliman ³, Assem Barakat ^{4,*}  and Ahmed A. M. Sarhan ⁵

¹ Chemistry Department, Faculty of Science, Suez Canal University, Ismailia 41522, Egypt; mohamed_gomaa@science.suez.edu.eg (M.F.Y.); ahmed_tawfeek83@yahoo.com or ahmed_boraie@science.suez.edu.eg (A.T.A.B.)

² Department of Chemistry, University of Jyväskylä, P.O. Box 35, FI-40014 Jyväskylä, Finland; matti.o.haukka@jyu.fi

³ Chemistry Department, Faculty of Science, Alexandria University, P.O. Box 426, Alexandria 21321, Egypt; saeed.soliman@alexu.edu.eg

⁴ Department of Chemistry, College of Science, King Saud University, P.O. Box 2455, Riyadh 11451, Saudi Arabia

⁵ Chemistry Department, Faculty of Science, Arish University, Al-Arish 45511, Egypt; ahmed_sarhan252@yahoo.com

* Correspondence: eidsalama2000@gmail.com or eid_mohamed@science.suez.edu.eg (E.E.S.); ambarakat@ksu.edu.sa (A.B.); Tel.: +966-11467-5901 (A.B.); Fax: +966-11467-5992 (A.B.)

Abstract: The regiospecific *S*-benzylation/allylation of two 4-aryl-5-indolyl-1,2,4-triazole-3-thione precursors was carried out using Et₃N as a base. Allyl group migration from exocyclic sulfur to the triazole nitrogen (N3) was successfully achieved in a short time via thermal fusion without the need for any catalyst. The allylation of indole nitrogen, along with exocyclic sulfur or triazole nitrogen (N3), was carried out using K₂CO₃ as stronger base. *S,N*-Diallylated products were converted to *N,N*-diallylated analogues using a simple fusion approach. Structural analyses of the two newly synthesized hybrids **2b** and **5b** investigated via the X-ray diffraction of a single crystal combined with Hirshfeld calculations. The compound **5b** was crystallized in a monoclinic crystal system and the *P*2₁/*c* space group, whereas in compound **2b**, the crystal system comprises the less symmetric triclinic and *P* – 1 space group. The asymmetric unit contains one and two molecules of **5b** and **2b**, respectively, while the unit cell contains four molecules in both cases. Hirshfeld analysis was performed in both systems to analyze the non-covalent interactions that control molecular packing. For **5b**, C...H, N...H, S...H, Cl...N and H...H interactions are the most significant. Their percentages are 23.7, 8.8, 4.5, 1.2 and 48.2, respectively. In the case of **2b**, the Cl...C, S...N, C...H, H...H and N...H interactions have the upper hand in molecular packing. In one unit, the percentages of these contacts are 2.3, 0.9, 26.8, 38.7 and 9.3%, while in the other unit, the corresponding values are 4.4, 1.3, 22.1, 43.6 and 9.0%, respectively.

Keywords: allylation; 1,2,4-triazole-3-thione; thio-aza allyl rearrangement; X-ray single-crystal analysis



Citation: Salama, E.E.; Youssef, M.F.; Boraie, A.T.A.; Haukka, M.; Soliman, S.M.; Barakat, A.; Sarhan, A.A.M. Base-Controlled Regiospecific Mono-Benzoylation/Allylation and Diallylation of 4-Aryl-5-indolyl-1,2,4-triazole-3-thione: Thio-Aza Allyl Rearrangement. *Crystals* **2023**, *13*, 992. <https://doi.org/10.3390/cryst13070992>

Academic Editor: Ulli Englert

Received: 24 May 2023

Revised: 14 June 2023

Accepted: 15 June 2023

Published: 21 June 2023



Copyright: © 2023 by the authors. Licensee MDPI, Basel, Switzerland. This article is an open access article distributed under the terms and conditions of the Creative Commons Attribution (CC BY) license (<https://creativecommons.org/licenses/by/4.0/>).

1. Introduction

Indole is a privileged structure and well known in the fields of chemistry and other disciplines due to its various applications in medicine, agrochemicals, and the industry [1]. In drug discovery, this indole motif has shown a high efficacy against [2] several types of cancers, including MCF-7 (breast cancer) [3], HepG-2 (human liver) and MOLT3 (T lymphoblast) cancer cells [4]; MES-SA/DX5 (human uterine sarcoma) and HCT15/CL02 (human colorectal) as multidrug resistant cancer cells [5]; and many other cancer type cell lines [6–8]. Enhanced biological activity has been reported in a combination of the

indole scaffold and other pharmacophores, such as heterocycles [9,10] (e.g., thiazoles, triazoles, oxadiazole, etc.) or a functional group of sulphonamides [11,12]. The indole scaffold not only has a high efficacy against cancer but many other forms of biological activity, such as anti-microbial [13], anti-malarial [14], anti-HIV [15], anti-convulsant [16], anti-inflammatory [17], anti-vascular [18], anti-diabetes (as they are α -glucosidase inhibitor agents) [19], etc. [20–24].

The combination of the triazole motif with the indole scaffold has recently received great attention in drug discovery development due to the many important pharmacological applications of the triazole unit [25–28], as well as recently discovered compounds. Nowadays, drugs containing the triazole nucleus are available on the market, for example, Fluconazole, Maraviroc, and Letrozole and others. These triazoles work as corrosion inhibitors [29] and dentate ligands due to their coordination chemistry with fluorescent applications [30].

Many examples regarding the attachment of the indole ring to triazoles have been reported. This has been identified as an anti-cancer agent targeting pro-apoptotic Bcl-2-inhibitory [31] or EGFR and Akt inhibitors [22], as well as a PARP-1 active agent [24]. To synthesize a new material with divergent functionalities is an interesting challenge for many chemists.

Based on these findings and the continuation of our research program [32], we synthesized new S-alkylated products, as well as N-alkylated products derived from the combination of the indole scaffold and triazole core structure. The explored and assigned molecular structure is based on single-crystal X-ray diffraction analysis and Hirshfeld analysis study.

In this study, we successfully achieved regiospecific mono-allylation and regiospecific di-allylation. NMR and single-crystal X-ray diffraction analysis were efficiently used for structural analysis.

2. Materials and Methods

Melting points were determined using melting-point apparatus (SMP10) in open capillaries and remained uncorrected. Chemicals, reagents and solvents were purchased from Alfa Aesar and Sigma-Merck. The progress of reactions and purity of products were observed using thin-layer chromatography (TLC) on pre-coated plates with silica gel 60 F₂₅₄ at a thickness of 0.25 mm (Merck). Nuclear magnetic resonance spectra (¹H NMR and ¹³C NMR) were determined in CDCl₃ and DMSO-*d*₆ and recorded using Bruker AC 400 MHz spectrometers with TMS as an internal reference standard. δ (ppm) was used for chemical shift description and values of coupling constants were given in Hz. HREI mass spectra were recorded with a Finnigan MAT 95XP instrument. CHNS-microanalysis performed on a Flash EA-1112 instrument.

2.1. General Procedures

2.1.1. Method a: Synthesis of the S-Alkylated Products

The selected 4-aryl-triazole-thiones **1a–b** (1.0 mmol) and Et₃N (1.1 mmol) in dry acetone (10 mL) was stirred for one hour, benzyl bromide or allyl bromide (1.1 mmol) was added portion-wise, and stirring was continued overnight. The solvent was removed under vacuum, water was added, and the formed precipitates were collected, dried and recrystallized from ethanol.

3-(Benzylsulfanyl)-4-phenyl-5-(1*H*-indol-2-yl)-1,2,4-triazole (**2a**)

Yield: 70%, m.p. 248–249 °C. ¹H NMR (400 MHz, DMSO-*d*₆): δ 4.42 (s, 2H), 5.59 (d, 1H, $J = 1.3$ Hz), 6.95 (t, 1H, $J = 7.4$ Hz), 7.15 (t, 1H, $J = 7.6$ Hz), 7.27–7.45 (m, 9H), 7.61–7.70 (m, 3H), 11.97 (s, 1H); ¹³C NMR (100 MHz, DMSO-*d*₆) δ 37.21, 101.89, 112.31, 120.20, 121.17, 123.60, 124.33, 127.65, 128.00, 128.39, 128.97, 129.45, 130.62, 131.10, 134.16, 137.00, 137.43, 149.67, 151.76; Elemental Analysis Calc. for [C₂₃H₁₈N₄S]: C, 72.23; H, 4.74; N, 14.65; S, 8.38 found C, 72.35; H, 4.79; N, 14.53; S, 8.49.

3-(Benzylsulfanyl)-4-(4-chlorophenyl)-5-(1H-indol-2-yl)-1,2,4-triazole (2b)

Yield: 65%, m.p. 242–243 °C. ¹H NMR (400 MHz, DMSO-*d*₆): δ 4.42 (s, 2H), 5.70 (s, 1H), 6.97 (t, 1H, *J* = 7.1 Hz), 7.16 (t, 1H, *J* = 7.2 Hz), 7.21–7.56 (m, 9H), 7.62–7.81 (m, 2H), 11.97 (s, 1H); ¹³C NMR (CDCl₃, 100 MHz) δ 37.37, 101.04, 112.31, 120.24, 121.33, 123.68, 124.13, 127.67, 128.04, 128.99, 129.46, 130.38, 130.71, 133.04, 135.75, 137.01, 137.39, 149.59, 151.69; Elemental Analysis Calc. for [C₂₃H₁₇ClN₄S]: C, 66.26; H, 4.11; Cl, 8.50; N, 13.44; S, 7.69 found C, 66.12; H, 4.28; Cl, 8.38; N, 13.48; S, 7.83.

3-(All-1-ylsulfanyl)-4-phenyl-5-(1H-indol-2-yl)-1,2,4-triazole (3a)

Yield: 81%, m.p. 218–219 °C [Lit. [24], 214–216 °C]. ¹H NMR (400 MHz, CDCl₃): δ 3.96 (d, H, *J* = 6.8 Hz), 5.20 (d, 1H, *J*_{cis} = 9.9 Hz), 5.34 (d, 1H, *J*_{trans} = 16.9 Hz), 5.78 (s, 1H), 5.95–6.05 (m, 1H), 7.06 (dd, 1H, *J* = 7.7, *J* = 8.0 Hz), 7.25 (dd, 1H, *J* = 7.7, *J* = 8.0 Hz), 7.36–7.96 (m, 7H), 11.05 (br.s, 1H); ¹³C NMR (CDCl₃, 100 MHz) δ 35.48, 102.74, 112.49, 119.12, 120.14, 120.99, 123.73, 127.78, 127.97, 130.29, 130.73, 132.61, 133.94, 136.93, 149.89, 152.34; HRMS (EI) calcd for C₁₉H₁₆N₄S (M⁺): 332.1096. Found: 332.1090.

3-(All-1-ylsulfanyl)-4-(4-chlorophenyl)-5-(1H-indol-2-yl)-1,2,4-triazole (3b)

Yield: 79%, m.p. 229–230 °C. ¹H NMR (400 MHz, CDCl₃): δ 3.95 (d, 2H, *J* = 7.0 Hz), 5.20 (d, 1H, *J*_{cis} = 10.0 Hz), 5.34 (d, 1H, *J*_{trans} = 16.9 Hz), 5.82 (s, 1H), 5.93–6.03 (m, 1H), 7.08 (t, 1H, *J* = 7.4 Hz), 7.26 (t, 1H, *J* = 7.6 Hz), 7.38 (d, 2H, *J* = 8.5 Hz), 7.47 (d, 1H, *J* = 8.0 Hz), 7.64 (d, 3H, *J* = 8.5 Hz), 10.64 (br.s, 1H); ¹³C NMR (CDCl₃, 100 MHz) δ 35.53, 102.65, 112.08, 119.24, 120.32, 121.10, 123.38, 123.94, 127.70, 129.25, 130.58, 132.28, 132.36, 136.64, 136.87, 149.58, 152.27; HRMS (EI) calcd for [C₁₉H₁₅N₄SCl]: 366.0706. Found: 366.0730.

2.1.2. Method b: Fusion of the Allyl-sulfanyl Isomers (Synthesis of the N-Allylated 4a–b and N,N-Diallylated Compounds 6a–b)

Separately, the S-allylated compounds from 3a–b (1.0 mmol) and S,N-diallylated compounds 5a–b (1.0 mmol) were fused at temperatures just higher than the respective melting point for few minutes (about 5 min) until all S-allyl starting materials were converted to N-allyl analogues as monitored by TLC. The products were purified by recrystallization from EtOH.

2-(All-1-yl)-4-phenyl-5-(1H-indol-2-yl)-3-thioxo-1,2,4-triazole (4a)

Yield: 76%, m.p. 165–166 °C. ¹H NMR (400 MHz, CDCl₃): δ 5.00 (d, 2H, *J* = 6.0 Hz), 5.42 (d, 1H, *J*_{cis} = 10.2 Hz), 5.47 (d, 1H, *J*_{trans} = 17.2 Hz), 5.77 (s, 1H), 6.05–6.24 (m, 1H), 7.09 (t, 1H, *J* = 7.4 Hz), 7.27 (t, 1H, *J* = 7.4 Hz), 7.32–7.53 (m, 4H), 7.67–7.68 (m, 3H), 8.94 (br.s, 1H); ¹³C NMR (CDCl₃, 100 MHz) δ 51.94, 105.26, 111.23, 119.76, 120.85, 121.73, 122.05, 124.93, 127.54, 128.61, 130.24, 130.70, 134.97, 136.24, 144.04, 168.65; HRMS (EI) calcd for [C₁₉H₁₆N₄S]: 332.1096. Found: 332.1091.

2-(All-1-yl)-4-(4-chlorophenyl)-5-(1H-indol-2-yl)-3-thioxo-1,2,4-triazole (4b)

Yield: 74%, m.p. 187–188 °C. ¹H NMR (400 MHz, CDCl₃): δ 4.97 (d, 2H, *J* = 6.0 Hz), 5.41 (dd, 1H, *J*_{cis} = 10.0, *J*_{gem} = 0.8 Hz), 5.44 (dd, 1H, *J*_{trans} = 17.2, *J*_{gem} = 0.8 Hz), 5.87 (d, 1H, *J* = 1.2 Hz), 6.10–6.18 (m, 1H), 7.07 (dd, 1H, *J* = 8.0, *J* = 7.2 Hz), 7.25 (dd, 1H, *J* = 7.2, *J* = 8.0 Hz), 7.33–7.38 (m, 3H), 7.45 (d, 1H, *J* = 8.0 Hz), 7.59 (d, 2H, *J* = 8.4 Hz), 8.96 (br.s, 1H); ¹³C NMR (CDCl₃, 100 MHz) δ 51.99, 105.26, 111.25, 119.90, 121.00, 121.82, 125.11, 127.50, 130.04, 130.56, 130.67, 133.38, 136.27, 136.79, 143.80, 168.66; HRMS (EI) calcd for [C₁₉H₁₅N₄SCl]: 366.0706. Found: 366.0716.

2.1.3. Method c: Synthesis of S,N-Diallylated Compounds 5a–b and N,N-Diallylated Compounds 6a–b

Separately, (1.0 mmol) of the selected hit compounds 3-allylsulfanyl-4-aryl-triazole-thiones 3a–b/2-(Allyl)-4-phenyl-5-indolyl-3-thioxo-1,2,4-triazoles 4a–b and anhydrous K₂CO₃ (1.1 mmol) in dry acetone (10 mL) were stirred for one hour, allyl bromide (1.1 mmol) was added portion-wise and all mixtures were stirred overnight (reaction progress was

monitored using TLC). Acetone was removed under vacuum, water was added, and the formed precipitates were collected, dried and recrystallized from ethanol.

3-(All-1-ylsulfanyl)-5-((1-all-1-yl)-indol-2-yl)-4-phenyl-1,2,4-triazole (**5a**)

Yield: 51%, m.p. 116–117 °C [Lit. [24], 113–114 °C]. ¹H NMR (400 MHz, CDCl₃): δ 3.92 (d, 2H, *J* = 7.2 Hz), 4.84 (d, 1H, *J*_{trans} = 17.2 Hz), 5.07 (d, 1H, *J*_{cis} = 10.4 Hz), 5.14 (d, 1H, *J*_{cis} = 10.0 Hz), 5.275–5.32 (m, 3H), 5.95–6.04 (m, 3H), 7.03 (dd, 1H, *J* = 8.0, *J* = 7.2 Hz), 7.19–7.24 (m, 3H), 7.33 (d, 1H, *J* = 8.4 Hz), 7.38 (d, 1H, *J* = 8.0 Hz), 7.47–7.52 (m, 3H); ¹³C NMR (CDCl₃, 100 MHz) δ 35.22, 47.10, 105.51, 110.44, 116.12, 119.10, 120.24, 121.36, 123.47, 124.59, 126.95, 127.65, 130.00, 130.20, 132.58, 134.14, 137.73, 149.05, 152.30; HRMS (EI) calcd for [C₂₂H₂₀N₄S]: 372.1409. Found: 372.1422.

3-(All-1-ylsulfanyl)-5-((1-all-1-yl)-indol-2-yl)-4-(4-chlorophenyl)-1,2,4-triazole (**5b**)

Yield: 47%, m.p. 160–161 °C. ¹H NMR (400 MHz, CDCl₃): δ 3.92 (d, 2H, *J* = 7.2 Hz), 4.82 (d, 1H, *J*_{trans} = 17.2, *J*_{gem} = 0.8 Hz), 5.06 (d, 1H, *J*_{cis} = 10.0, *J*_{gem} = 0.8 Hz), 5.15 (d, 1H, *J*_{cis} = 9.6 Hz), 5.28–5.33 (m, 3H), 5.95–6.04 (m, 3H), 7.06 (dd, 1H, *J* = 8.0, *J* = 7.2 Hz), 7.17 (d, 2H, *J* = 8.8 Hz), 7.23 (dd, 1H, *J* = 7.2, *J* = 8.0 Hz), 7.34 (d, 1H, *J* = 8.0 Hz), 7.43 (d, 1H, *J* = 8.0 Hz), 7.47 (d, 2H, *J* = 8.4 Hz); ¹³C NMR (CDCl₃, 100 MHz) δ 35.43, 47.04, 105.85, 110.46, 116.22, 119.22, 120.43, 121.45, 123.76, 124.01, 126.93, 128.95, 130.31, 132.31, 132.48, 134.06, 136.45, 137.89, 148.85, 152.25; HRMS (EI) calcd for C₂₂H₁₉N₄SCl (M⁺): 406.1019. Found: 406.1022.

2-(All-1-yl)-5-((1-all-1-yl)-indol-2-yl)-4-phenyl-3-thioxo-1,2,4-triazole (**6a**)

Yield: 73_{method b}, 55_{method c}%, m.p. 145–146 °C. ¹H NMR (400 MHz, CDCl₃): δ 4.89 (d, 1H, *J*_{trans} = 17.2 Hz), 5.02 (d, 2H, *J* = 6.0 Hz), 5.08–5.12 (m, 3H), 5.36 (d, 1H, *J*_{cis} = 10.4, *J*_{gem} = 0.8 Hz), 5.42 (d, 1H, *J*_{trans} = 17.2, *J*_{gem} = 0.8 Hz), 5.85–5.94 (m, 1H), 6.01 (s, 1H), 6.05–6.12 (m, 1H), 7.05 (dd, 1H, *J* = 8.0, *J* = 7.2 Hz), 7.23–7.32 (m, 4H), 7.40 (d, 1H, *J* = 0.8 Hz), 7.50–7.60 (m, 3H); ¹³C NMR (CDCl₃, 100 MHz) δ 47.02, 51.92, 107.80, 110.34, 116.66, 119.74, 120.66, 121.78, 122.91, 124.29, 126.70, 128.47, 129.85, 130.10, 130.80, 133.58, 135.28, 137.99, 143.63, 168.09; HRMS (EI) calcd for [C₂₂H₂₀N₄S]: 372.1409. Found: 372.1390.

2-(All-1-yl)-5-((1-all-1-yl)-indol-2-yl)-4-(4-chlorophenyl)-3-thioxo-1,2,4-triazole (**6b**)

Yield: 69_{method b}, 51_{method c}%, m.p. 174–175 °C. ¹H NMR (400 MHz, CDCl₃): δ 4.88 (d, 1H, *J*_{trans} = 17.1 Hz), 5.00 (d, 2H, *J* = 5.9 Hz), 5.09–5.14 (m, 3H), 5.42 (d, 1H, *J*_{cis} = 10.4 Hz), 5.46 (d, 1H, *J*_{trans} = 17.2 Hz), 5.90–5.97 (m, 1H), 6.11–6.18 (m, 2H), 7.13 (t, 1H, *J* = 7.4 Hz), 7.29–7.51 (m, 7H); ¹³C NMR (CDCl₃, 100 MHz) δ 46.95, 51.92, 107.80, 110.31, 116.69, 119.85, 120.76, 121.81, 122.55, 124.42, 126.61, 129.76, 130.11, 130.59, 133.47, 133.64, 136.10, 137.97, 143.36, 168.03; HRMS (EI) calcd for C₂₂H₁₉N₄SCl (M⁺): 406.1019. Found: 406.1023.

2.2. Crystal Structure Determination

The technical method for determining crystal structures for compounds **5b** and **2b** is provided in supporting information [33–36], and crystal data are summarized in Table 1.

Table 1. Crystal data.

	5b	2b
CCDC no.	2,264,129	2,264,130
empirical formula	C ₂₂ H ₁₉ ClN ₄ S	C ₂₃ H ₁₇ ClN ₄ S
fw	406.92	416.92
temp (K)	120 (2)	120 (2)
λ (Å)	0.71073	1.54184
cryst syst	Monoclinic	Triclinic
space group	<i>P</i> 2 ₁ / <i>c</i>	<i>P</i> 1
<i>a</i> (Å)	11.0242 (3)	12.1537 (5)
<i>b</i> (Å)	16.5074 (4)	12.8679 (5)

Table 1. Cont.

	5b	2b
<i>c</i> (Å)	11.0507 (2)	15.0994 (5)
α (deg)	90	70.272 (3)
β (deg)	97.688 (2)	69.417 (3)
γ (deg)	90	67.402 (4)
<i>V</i> (Å ³)	1992.94(8)	1984.17 (15)
<i>Z</i>	4	4
ρ_{calc} (mg/m ³)	1.356	1.396
μ (Mo K α) (mm ⁻¹)	0.312	2.818
No. reflns.	23,307	53,703
Completeness to theta = 25.242°	100%	
Completeness to theta = 67.684°		100%
Unique reflns.	6619	8329
GOOF (<i>F</i> ²)	1.037	1.034
<i>R</i> _{int}	0.0475	0.0342
<i>R</i> ₁ ^a (<i>I</i> ≥ 2σ)	0.0461	0.0296
<i>wR</i> ₂ ^b (<i>I</i> ≥ 2σ)	0.1106	0.0747

$$^a R_1 = \sum ||F_o| - |F_c|| / \sum |F_o|. \quad ^b wR_2 = [\sum [w(F_o^2 - F_c^2)^2] / \sum [w(F_o^2)^2]]^{1/2}.$$

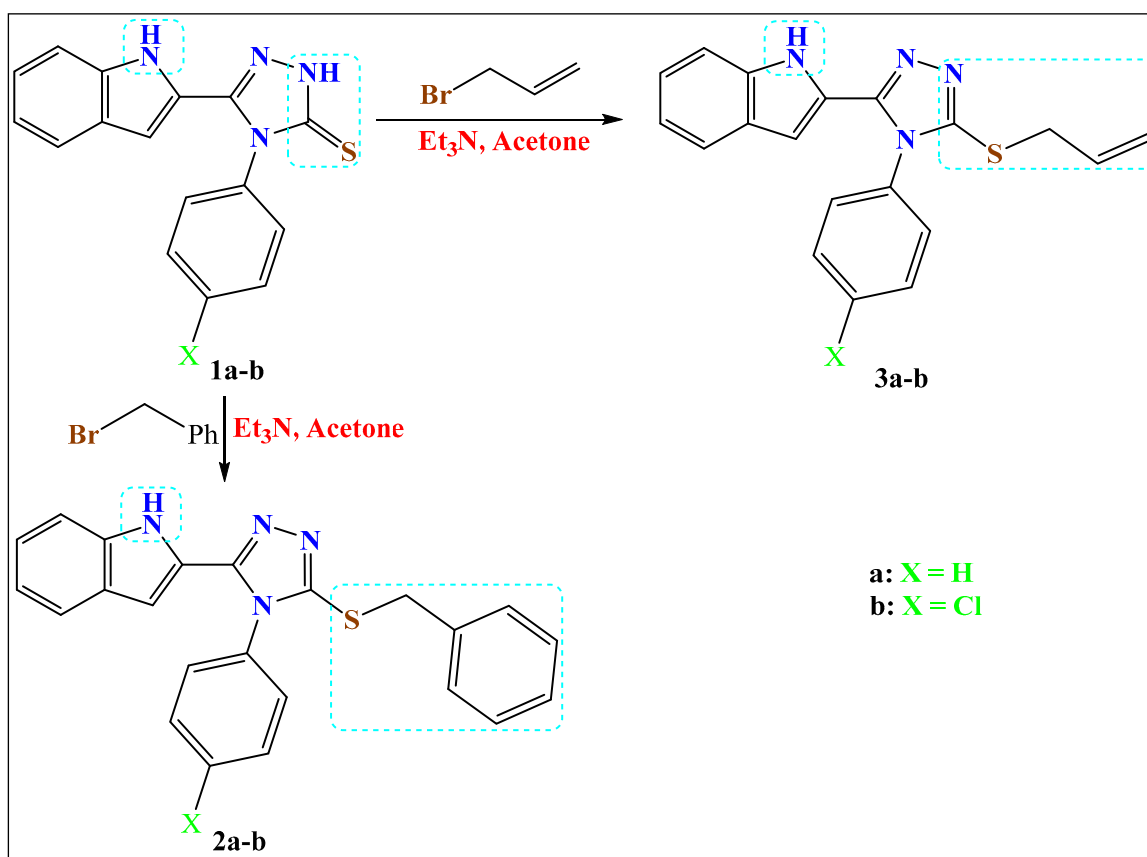
2.3. Hirshfeld Surface Analysis

Topology analyses were performed using Crystal Explorer 17.5 program [37].

3. Results and Discussion

The regiospecific *S*-benzylzation and *S*-allylation of 5-indolyl-4-phenyl-1,2,4-triazole-3-thione **1a** and its 4-(4-chlorophenyl) analogue **1b** were successfully performed via reaction with benzyl bromide and allyl bromide, respectively. This reaction was promoted by an Et₃N base, which was used as a catalyst in an acetone medium (Scheme 1). ¹H NMR and ¹³C NMR spectroscopy revealed the following characteristic signals that support structural assignments: benzylated products **2a–b** spectra contained methylene protons of the benzyl group (-CH₂Ph) (almost at 4.42 ppm), and the respective methylene carbons were approximately at 37.30 ppm. The allylated compounds **3a–b** had allylic protons (attached to saturated sp³ carbon -S-CH₂) as a doublet at 3.95 ppm, while the corresponding allylic carbon appeared to be near 35.50 ppm. In addition, the ¹H NMR of **3a–b** displayed the *cis* protons of the vinylic methylene group at 5.20 ppm with a coupling constant value of ³*J* ≈ 10.0 Hz, whereas the *trans* proton was found at 5.34 ppm with ³*J* ≈ 16.9 Hz. The remaining vinylic CH proton was found as multiplet in the region at 5.95–6.05 ppm. The two triazole carbons in the four compounds **2a–b**, **3a–b** were detected near 149.00 and 152.00 ppm.

Moreover, a simple, efficient and catalyst-free thermal rearrangement of the allyl moiety from exocyclic sulfur to N(2) of the triazole ring was successfully carried out via the fusion of *S*-allylated compounds **3a–b** on a hotplate for a few minutes at temperatures just higher than their melting points to yield *N*-allylated compounds **4a–b**. The *S*-allylated triazoles **3a–b** were further allylated in the presence of the K₂CO₃ base, which catalyzed the allylation of indole nitrogen to afford the *S,N*-diallylated products **5a–b**. To obtain *N,N*-diallylated products **6a–b**, the allylation of indole nitrogen and triazole nitrogen was regiospecifically carried out either via the allylation of *N*-allylated precursors **4a–b** or via the thermal thio-aza allyl rearrangement of **5a–b** (Scheme 2). The allyl group migration from sulfur to nitrogen was supported by NMR spectra of **4a–b**. The allylic methylene protons experienced a downfield chemical shift, appearing near 5.00 ppm where, the respective allylic methylene carbon shifted approximately to 51.90 ppm. In addition, one of the triazole carbon signals was shifted to 168.65 ppm, supporting C=S formation caused by allyl group migration.



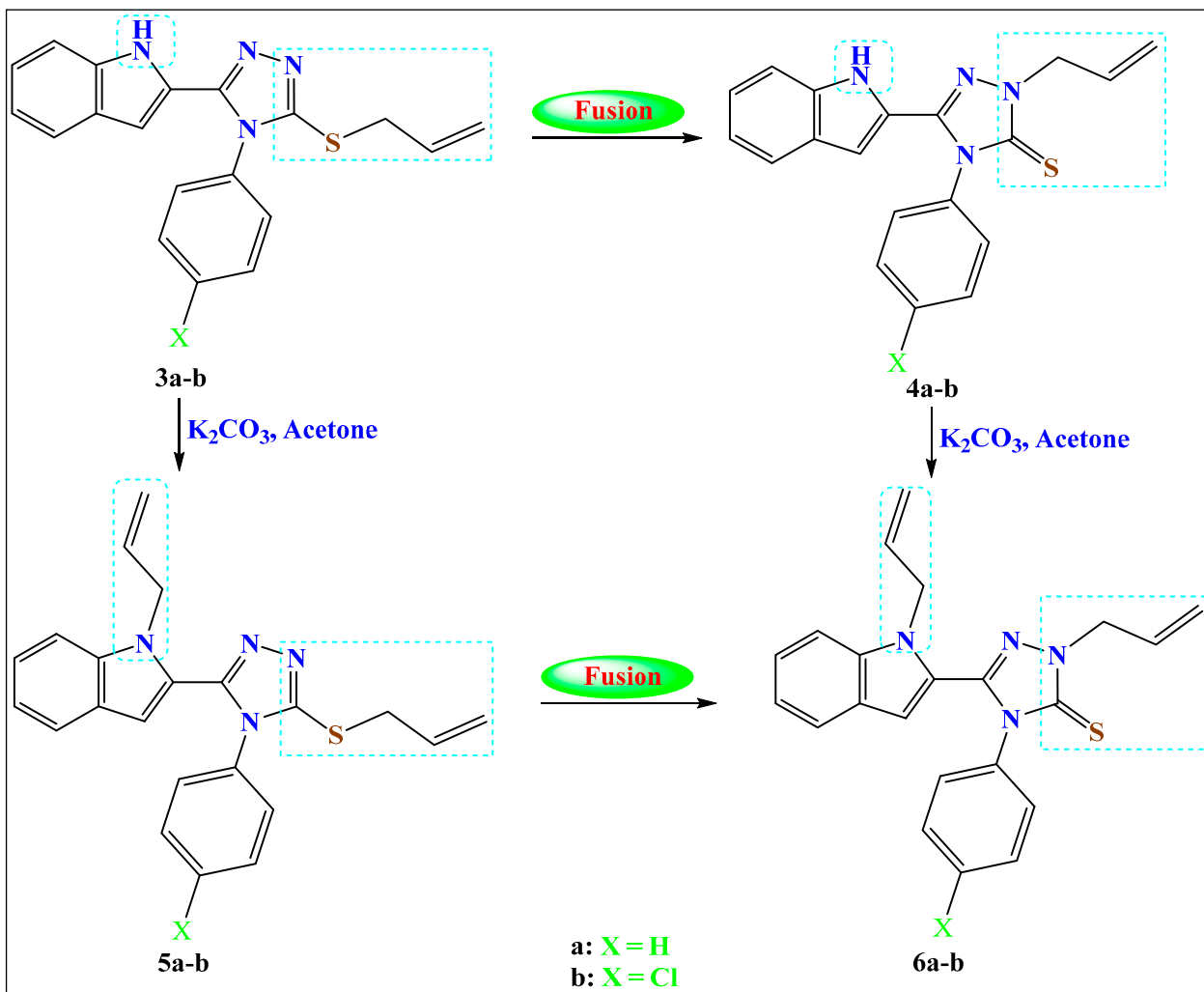
Scheme 1. Synthesis of compounds **2a–b** and **3a–b**.

Sulfur and indole nitrogen allylation in the compounds **5a–b**, was confirmed due to the disappearance of indole NH and the appearance of new allyl group signals. The S,N-diallyl methylene group protons signals were detected near 3.92 ppm (for SCH₂) and 4.84 ppm (NCH₂) and the respective carbons were detected at 35.22 ppm (for SCH₂) and 47.10 ppm (for NCH₂). The two triazole carbons were found near 149.00 and 152.00 ppm.

The allylation of indole nitrogen, along with triazole nitrogen **6a–b**, established based on NMR, which displayed the signals of the two allylic methylene groups near 4.89 ppm and 5.02 ppm and the respective allylic carbons found near 47.00 ppm and 52.00 ppm. Moreover, the appearance of a ¹³C NMR signal at 168.00 ppm strongly supports the thiocarbonyl group (C=S).

3.1. Crystal Structure Description

The structure of **5b** is shown in Figure 1, which is found to have a good agreement with the proposed structure based on the spectral characterizations. Selected bond distances are shown in Table 2, while selected bond angles are depicted in Table S1 (Supplementary Data). The structure solution of compound **5b** has unit cell parameters of $a = 11.0242$ (3) Å, $b = 16.5074$ (4) Å, $c = 11.0507$ (2), and $\beta = 97.688$ (2)°. Hence, the crystal system is monoclinic, while the space group is $P2_1/c$. The asymmetric formula is one unit, while $z = 4$. The crystal density is 1.356 Mg/m³, and the unit cell volume is 1992.94 (8) Å³. There are a number of aromatic ring systems in which the three planar ring systems are not coplanar with one another. The mean plane of the triazole moiety, and the phenyl moiety has an angle of 77.36 (12)°. Additionally, the mean plane of the indole and triazole moieties is also twisted, and the twist angle in this case is less than 35.98 (11)°.



Scheme 2. Synthesis of the target compounds 4–6.

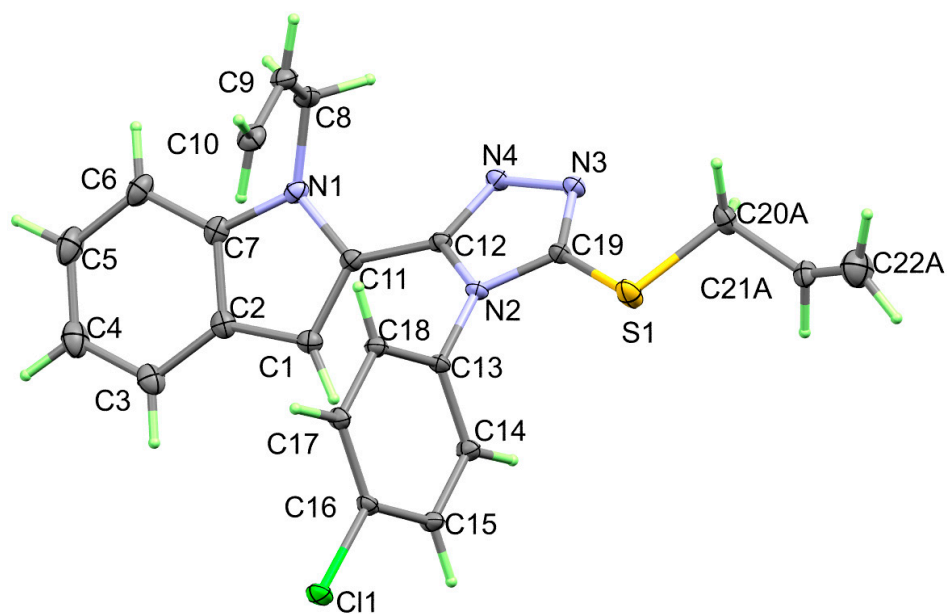


Figure 1. X-Ray structure of 5b.

Table 2. Bond lengths (Å) for **5b** and **2b**. ^a

Bond	Length/Å	Bond	Length/Å
5b		2b	
Cl(1)-C(16)	1.7389 (13)	Cl(1)-C(13)	1.7325 (13)
S(1)-C(19)	1.7418 (16)	S(1)-C(16)	1.7460 (14)
S(1)-C(20B)	1.8204 (16)	S(1)-C(17)	1.8318 (14)
S(1)-C(20A)	1.8204 (16)	N(1)-C(1)	1.3716 (18)
N(1)-C(7)	1.386 (2)	N(1)-C(8)	1.3788 (17)
N(1)-C(11)	1.3938 (19)	N(2)-C(16)	1.3740 (17)
N(1)-C(8)	1.457 (2)	N(2)-C(9)	1.3755 (17)
N(2)-C(19)	1.3732 (18)	N(2)-C(10)	1.4372 (16)
N(2)-C(12)	1.3802 (18)	N(3)-C(16)	1.3096 (17)
N(2)-C(13)	1.4364 (17)	N(3)-N(4)	1.3989 (16)
N(3)-C(19)	1.3124 (18)	N(4)-C(9)	1.3131 (17)
N(3)-N(4)	1.4027 (18)	Cl(1B)-C(13B)	1.7373 (13)
N(4)-C(12)	1.3190 (17)		

^a List of bond angles are given in Table S1 (Supplementary Materials).

The molecular units of **5b** are connected with each other via the N ... H and S ... H non-covalent contacts shown in Figure 2A. A list of the H-bond parameters is shown in Table 3. The donor–acceptor distances of these interactions are 3.456 (2) and 3.741 (6) Å for C14-H14 ... N4 and C22A-H22B ... S1, respectively. The packing scheme for the molecular units along the *ab* plane is shown in Figure 2B.

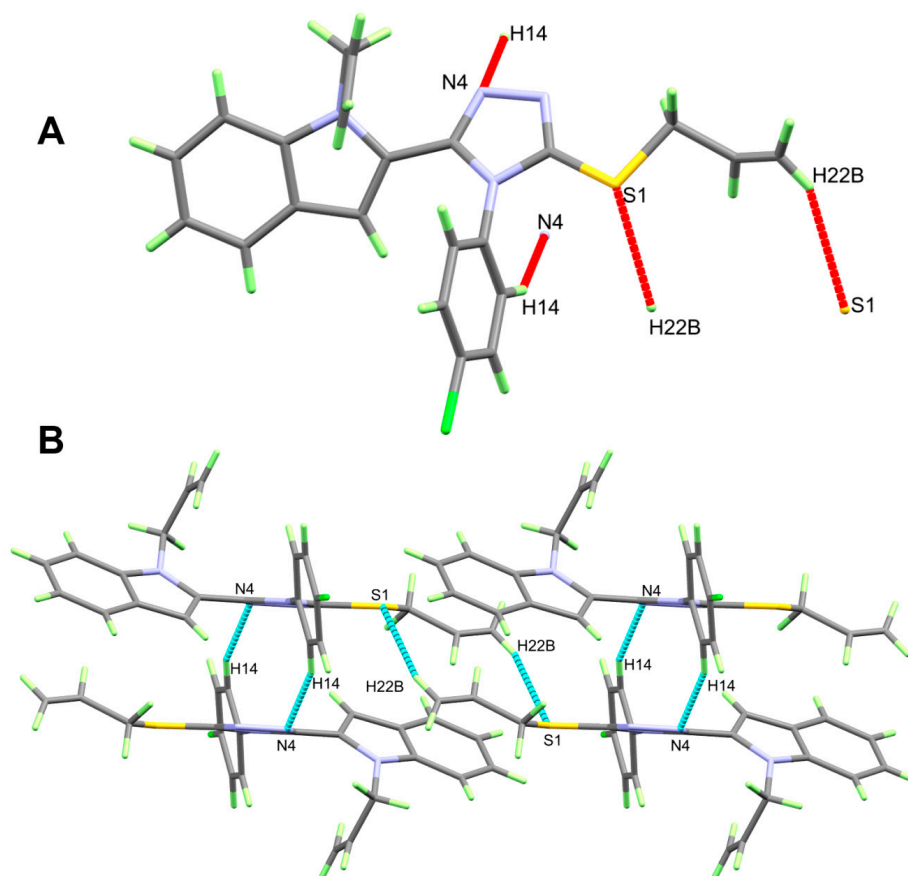
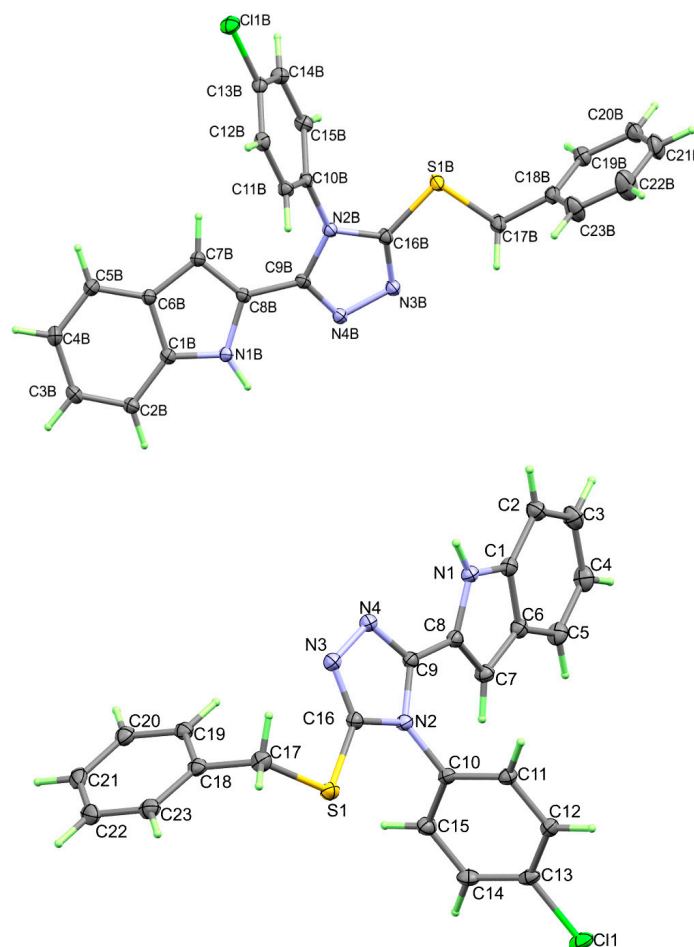
**Figure 2.** The N ... H/S ... H contacts (A) and packing view via N ... H/S ... H contacts (B) for **5b**.

Table 3. Hydrogen bonds for **2b** and **5b** [Å and °].

D-H ... A	d(D-H)	d(H ... A)	d(D ... A)	<(DHA)	Symm. Code
5b					
C14-H14 ... N4	0.95	2.58	3.456 (2)	154	1 - x, 1 - y, 1 - z
C22A-H22B ... S1	0.95	2.87	3.741 (6)	153	2 - x, 1 - y, 1 - z
2b					
C17-H17B ... N3	0.99	2.55	3.025 (2)	109	
C19-H19 ... N3	0.95	2.6	3.388 (2)	140	
N1-H1 ... N4B	0.86 (2)	2.08 (2)	2.913 (2)	164.1 (18)	
N1B-H1B ... N4	0.88 (2)	0.88 (2)	2.920 (2)	163.1 (18)	
C11-H11 ... N3	0.95	2.59	3.440 (2)	149	1 - x, 1 - y, 1 - z
C15B-H15B ... N1B	0.95	2.53	3.396 (2)	152	-x, 2 - y, 1 - z

The X-ray structure of **2b** is shown in Figure 3. Crystal data and a list of the geometric parameters are depicted in Tables 1 and 2, respectively. In this case, the crystal system is triclinic and the space group is *P*-1. The lattice parameters are $a = 12.1537$ (5) Å, $b = 12.8679$ (5) Å, $c = 15.0994$ (5) Å, $\alpha = 70.272$ (3)°, $\beta = 69.417$ (3)°, and $\gamma = 67.402$ (4)°. The asymmetric unit is two molecules of **2b**, while $z = 4$. The crystal density is 1.396 Mg/m³, and the unit cell volume is 1984.17 (15) Å³. In **2b**, the twist angles between the triazole ring and the Cl-phenyl or indole rings are smaller than in **5b**. For one molecule, the twist angles are 65.79 (10)° and 18.94 (12)°, respectively. The molecule with letter B in the atom numbering has twist angles of 75.34 (10)° and 21.40 (11)°, respectively.

**Figure 3.** Structure with atom numbering for **2b** drawn using 30% probability level for thermal ellipsoids.

The molecules of **2b** are interconnected in the crystal via the N ... H contacts, as depicted in Table 3 and Figure 4A. There are two types of non-covalent interactions: polar N-H ... N and non-polar C-H ... N. The polar hydrogen bonds, such as the N1-H1 ... N4B and N1B-H1B ... N4 have donor–acceptor distances of 2.913 (2) and 2.920 (2) Å, respectively. On the other hand, the C-H ... N interaction distances occurred at longer distances (3.025 (2)–3.440 (2) Å). The packing scheme for the molecular units of **2b** is shown in Figure 4B.

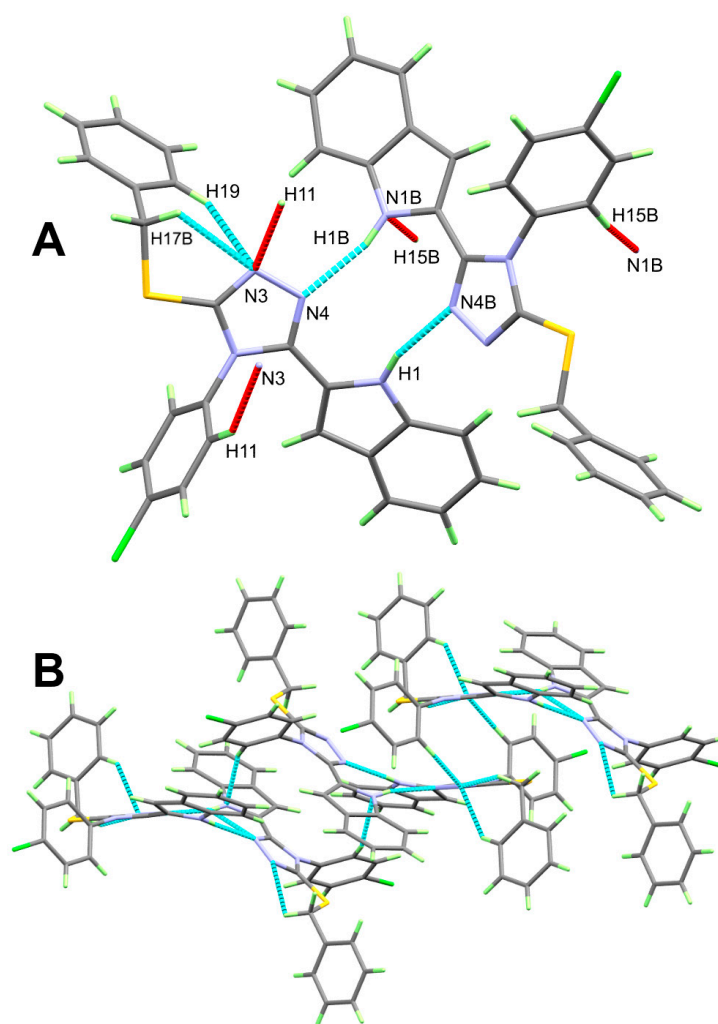


Figure 4. The N ... H contacts (A) and molecular packing via N ... H contacts (B) for **2b**.

3.2. Hirshfeld Surface Analysis

The analysis of intermolecular interactions in the crystal of **5b** is presented in Figure 5. The most dominant contacts are the H ... H (48.2%), C ... H (23.7%), Cl ... H (11.0%), N ... H (8.8%) and S ... H (4.5%). Other minor interactions such as Cl ... N (1.2%) and C ... N (1.1%) contacts were detected.

There are three important surfaces in the Hirshfeld analysis, which are shown in Figure 6. In the d_{norm} surface, the most important short contacts appeared as red spots. These red spots are related to C ... H, N ... H, S ... H, Cl ... N and H ... H interactions. A list of the shortest intermolecular contacts detected in the crystal of **5b** is shown in Table 4. The other two surfaces (shape index and curvedness maps) are important for inspecting the possibility of π - π stacking interactions. The absence of red and blue triangles in the shape index and flat areas of the curvedness map indicates the absence of π - π stacking interactions. In accordance with this observation, the %C ... C and %C ... N values are 0.7 and 1.1, respectively.

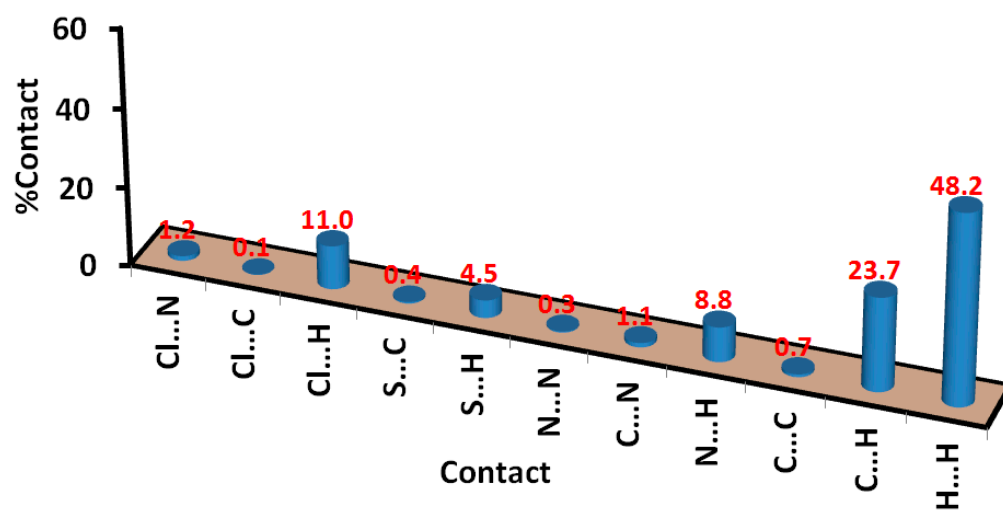


Figure 5. Contact percentages in 5b.

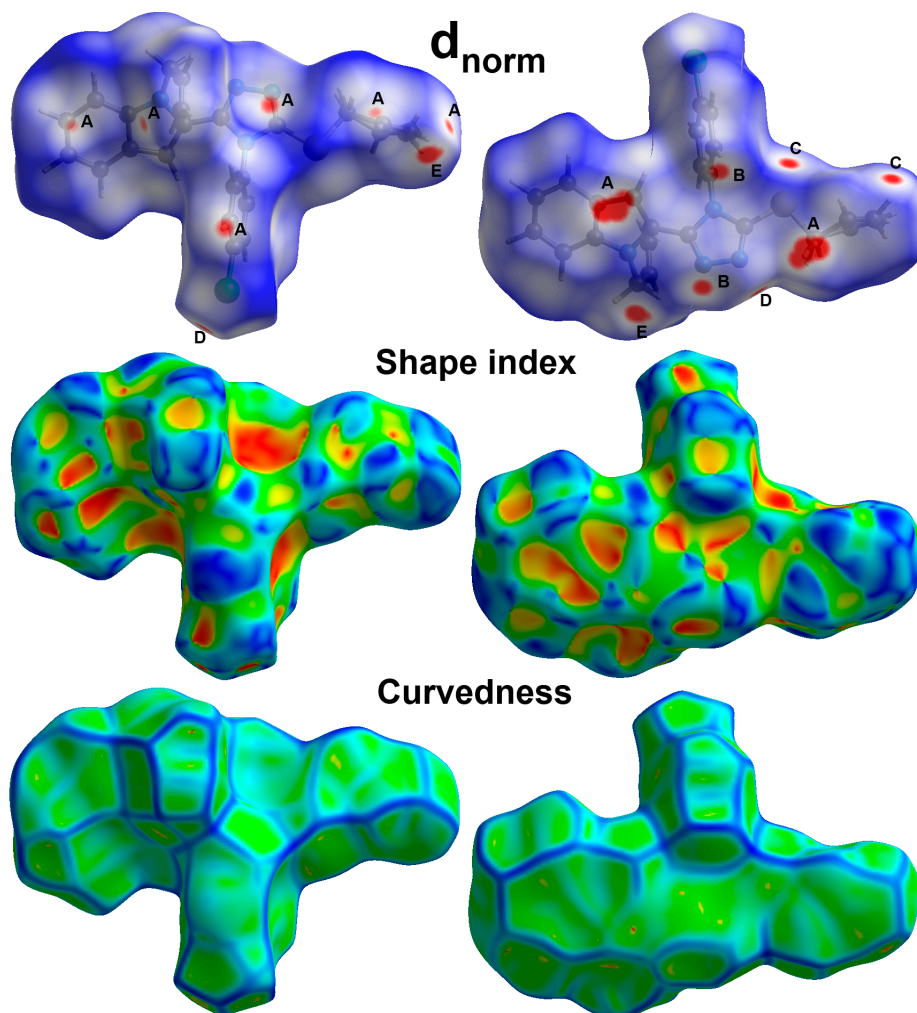
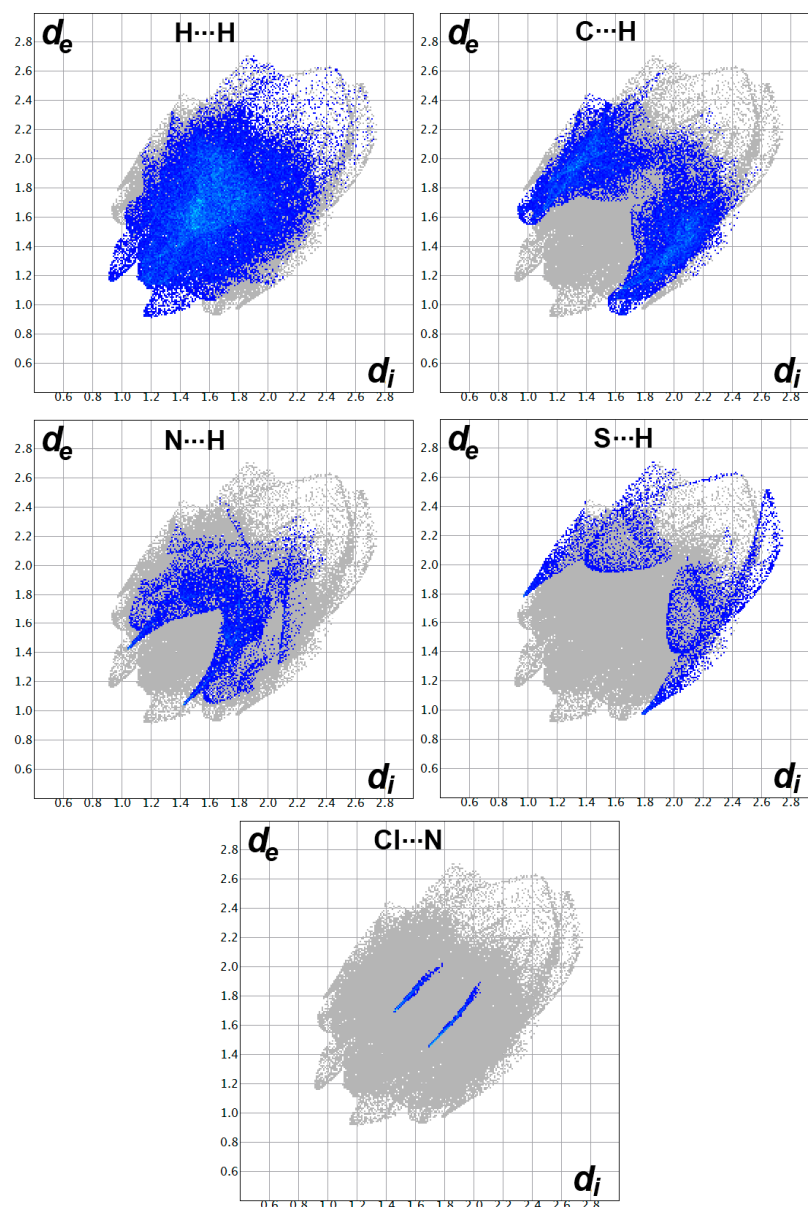


Figure 6. Hirshfeld surfaces of 5b: (A) C...H, (B) S...H, (C) Cl...N, (D) H...H.

Table 4. Short contacts in 5b.

Contact	Distance	Contact	Distance
H8B ... H22D	2.084	H20A ... C1	2.599
H22D ... C8	2.696	H17 ... C19	2.657
H22D ... C10	2.607	H21B ... C5	2.747
H5 ... C17	2.762	H14 ... N4	2.458
H20C ... C2	2.580	S1 ... H22B	2.754
H20C ... C1	2.531	Cl1 ... N3	3.149

In Figure 7, the fingerprint plots of the C ... H, N ... H, S ... H, Cl ... N and H ... H contacts are shown. The blue area in the fingerprint plot gave the percentage of each of these contacts, as shown in Figure 5. Additionally, the pattern of the fingerprint plot sheds light on the importance of intermolecular interactions. All contacts presented in Figure 7 appear as sharp spikes, indicating that these interactions have short interaction distances, mostly shorter than total vdWs radii of the interacting atoms.

**Figure 7.** Decomposed fingerprint plots for the short contacts in 5b.

In the case of the crystal structure of **2b**, the results indicate the presence of two molecules as asymmetric formula. Hence, two surfaces for each molecule are presented in Figure 8. Analysis of the different intermolecular interactions in this crystal structure is presented in Table 5.

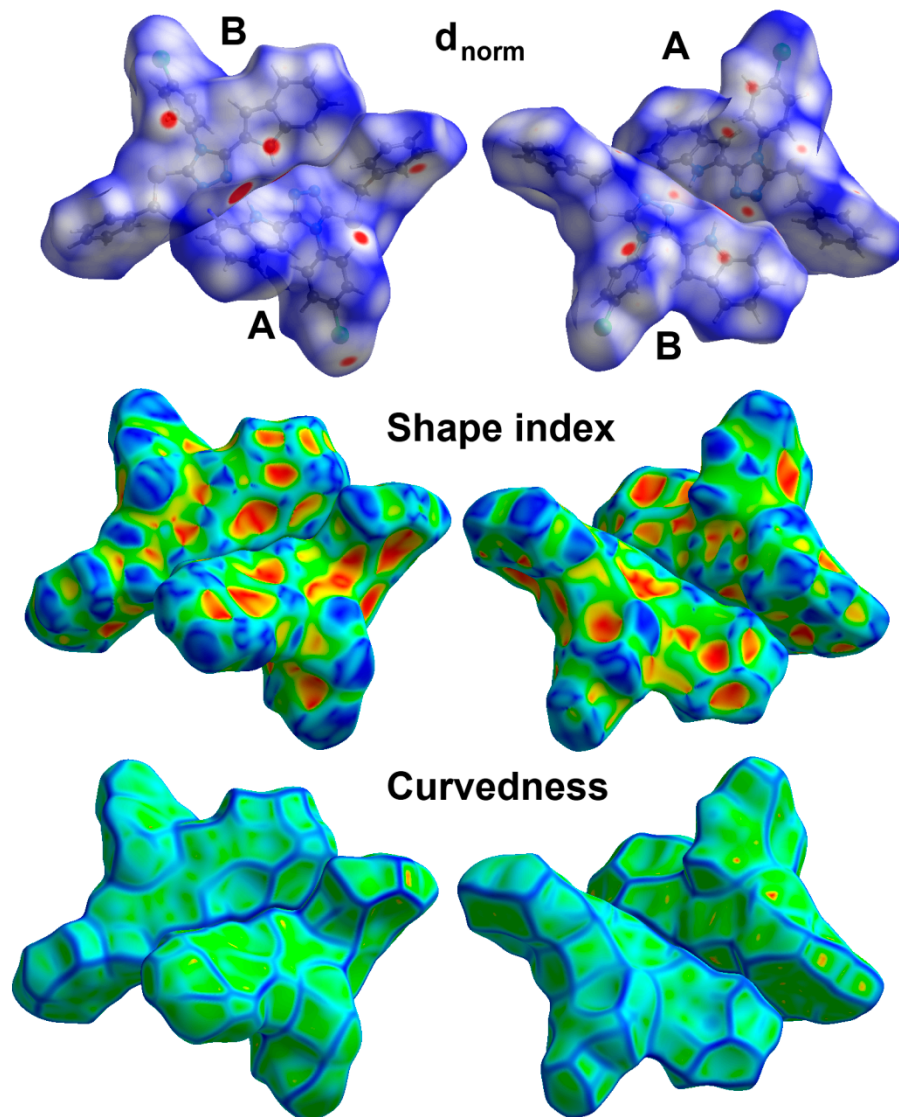


Figure 8. Hirshfeld surfaces of **2b**.

Table 5. The non-covalent interactions and their percentages in **2b**.

Contact	A	B
Cl ... S	0.0	0.3
Cl ... N	0.3	0.4
Cl ... C	4.4	2.3
Cl ... H	8.5	10.6
S ... N	1.3	0.9
S ... C	0.5	1.8
S ... H	5.8	3.2
N ... N	0.2	0.0
C ... N	1.7	1.5
N ... H	9.0	9.3

Table 5. Cont.

Contact	A	B
C ... C	2.7	4.2
C ... H	22.1	26.8
H ... H	43.6	38.7

It is clear from Table 5 that there are some differences in the intermolecular interactions that occurred in units A and B. In both units, H ... H, C ... H, Cl ... H and N ... H are the most dominant interactions. Further inspection of the d_{norm} map indicated the importance of Cl ... C, S ... N, C ... H, H ... H and N ... H interactions in the molecular packing of unit A, where all these interactions have the characteristics of short-distance interactions (Figure 9). The same is true for unit B, but Cl ... C interactions are less important in this case, constituting a major difference between the two units. All short interactions and their distances are listed in Table 6.

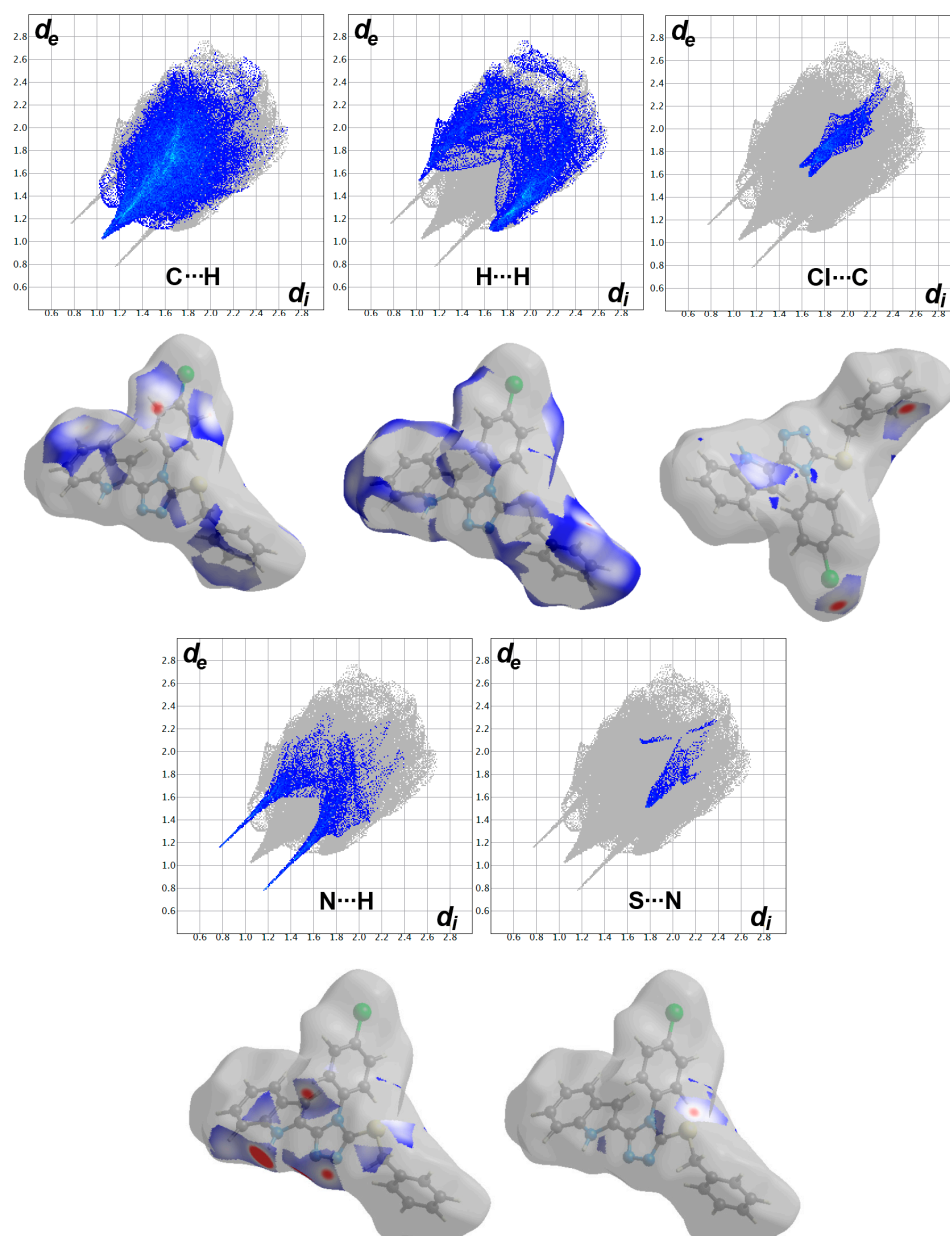
Figure 9. Decomposed d_{norm} and fingerprint plots for the short contacts in unit A of 2b.

Table 6. Short contacts in **2b**.

Contact	Distance	Contact	Distance
S1 ... N4B	3.289	H23 ... H17C	2.121
N4B ... H1	1.933	H19 ... H2B	2.075
N3 ... H11	2.479	C14 ... H11B	2.762
Cl1 ... C21	3.246	C19 ... H12B	2.756
H23 ... H17C	2.121	C19B ... H5	2.776
H19 ... H2B	2.075	C11B ... H15	2.567
H21 ... H5B	2.122		

Additionally, the presence of some C ... C and C ... N interactions of up to 4.2% and 1.7%, respectively, might indicate the presence of π - π stacking interactions. Actually, all C ... C and C ... N contacts have significantly longer interaction distances than the total vdWs radii of the interacting atoms. Additionally, the absence of π - π stacking interactions is evident from the curvedness and shape index maps.

4. Conclusions

The base used in the alkylation of 4-aryl-5-indolyl-1,2,4-triazole-3-thione precursors affects the structure of the final product. The regiospecific *S*-benzylation/ allylation occurred when Et₃N used. Thio-aza allyl rearrangement was successfully achieved *via* thermal fusion of *S*-allylated scaffolds. The indole nitrogen was allylated along with exocyclic sulfur or triazole nitrogen (N3) using K₂CO₃. *S,N*-diallylated products were transformed into *N,N*-diallylated analogues via thermal fusion. The structure of the two compounds was confirmed via the X-ray diffraction of a single crystal. Their supramolecular structures were calculated based on Hirshfeld calculations. The molecular packing of **5b** was found to be controlled by short C ... H (23.7%), N ... H (8.8%), S ... H (4.5%), Cl ... N (1.2%) and H ... H (48.2%) contacts. On the other hand, the supramolecular structure of **2b** depended on Cl ... C, S ... N, C ... H, H ... H and N ... H interactions. Their percentages are calculated to be 2.3–4.4, 0.9–1.3, 26.8–22.1, 38.7–43.6, 9.3–9.0, respectively.

Supplementary Materials: The following supporting information can be downloaded at: <https://www.mdpi.com/article/10.3390/cryst13070992/s1>, X-ray structure determinations; Table S1: Bond angles (°) for **2b** and **5b**.

Author Contributions: Conceptualization, E.E.S., A.T.A.B., A.A.M.S. and A.B.; methodology, E.E.S., A.A.M.S., A.T.A.B. and M.F.Y.; software, S.M.S. and M.H.; validation, E.E.S., A.T.A.B. and A.B.; formal analysis, M.F.Y., E.E.S. and A.T.A.B.; investigation, A.T.A.B.; resources, A.T.A.B. and A.B.; data curation, M.F.Y.; writing—original draft preparation, A.T.A.B.; writing—review and editing, E.E.S., A.T.A.B., A.B., S.M.S., M.F.Y., M.H. and A.A.M.S.; visualization, A.T.A.B. and A.B.; supervision, A.T.A.B.; project administration, A.B.; funding acquisition, A.B. All authors have read and agreed to the published version of the manuscript.

Funding: The paper was funded by Researchers Supporting Project (RSP2023R64), King Saud University, Riyadh, Saudi Arabia.

Data Availability Statement: Not applicable.

Acknowledgments: The authors would like to extend their sincere appreciation to the Researchers Supporting Project (RSP2023R64), King Saud University, Riyadh, Saudi Arabia.

Conflicts of Interest: The authors declare no conflict of interest.

References

1. Elshaier, Y.A.; Nemr, M.T.; Al Refaey, M.; Fadaly, W.A.; Barakat, A. Chemistry of 2-vinylindoles: Synthesis and applications. *New J. Chem.* **2022**, *46*, 13383–13400. [CrossRef]
2. Kochanowska-Karamyan, A.J.; Hamann, M.T. Marine indole alkaloids: Potential new drug leads for the control of depression and anxiety. *Chem. Rev.* **2010**, *110*, 4489–4497. [CrossRef]

3. Hong, C.; Firestone, G.L.; Bjeldanes, L.F. Bcl-2 family-mediated apoptotic effects of 3, 3'-diindolylmethane (DIM) in human breast cancer cells. *Biochem. Pharmacol.* **2002**, *63*, 1085–1097. [[CrossRef](#)] [[PubMed](#)]
4. Pingaew, R.; Prachayasittikul, S.; Ruchirawat, S.; Prachayasittikul, V. Synthesis and cytotoxicity of novel 2, 2'-bis- and 2, 2', 2''-tris-indolylmethanes-based bengacarboline analogs. *Arch. Pharm. Res.* **2012**, *35*, 949–954. [[CrossRef](#)] [[PubMed](#)]
5. Rahman, K.W.; Li, Y.; Wang, Z.; Sarkar, S.H.; Sarkar, F.H. Gene expression profiling revealed survivin as a target of 3, 3'-diindolylmethane-induced cell growth inhibition and apoptosis in breast cancer cells. *Cancer Res.* **2006**, *66*, 4952–4960. [[CrossRef](#)]
6. Yoo, M.; Choi, S.-U.; Choi, K.Y.; Yon, G.H.; Chae, J.-C.; Kim, D.; Zylstra, G.; Kim, E. Trisindoline synthesis and anticancer activity. *Biochem. Biophys. Res. Commun.* **2008**, *376*, 96–99. [[CrossRef](#)]
7. Safe, S.; Papineni, S.; Chintharlapalli, S. Cancer chemotherapy with indole-3-carbinol, bis (3'-indolyl) methane and synthetic analogs. *Cancer Lett.* **2008**, *269*, 326–338. [[CrossRef](#)]
8. Foderaro, T.A.; Barrows, L.R.; Lassota, P.; Ireland, C.M. Bengacarboline, a New β -Carboline from a Marine Ascidian *Didemnum* sp. *J. Org. Chem.* **1997**, *62*, 6064–6065. [[CrossRef](#)]
9. Nagarsenkar, A.; Prajapati, S.K.; Guggilapu, S.D.; Birineni, S.; Kotapalli, S.S.; Ummanni, R.; Babu, B.N. Investigation of triazole-linked indole and oxindole glycoconjugates as potential anticancer agents: Novel Akt/PKB signaling pathway inhibitors. *Med. Chem. Commun.* **2016**, *7*, 646–653. [[CrossRef](#)]
10. Kaminsky, D.; Bednarczyk-Cwynar, B.; Vasylenko, O.; Kazakova, O.; Zimenkovsky, B.; Zaprutko, L.; Lesyk, R. Synthesis of new potential anticancer agents based on 4-thiazolidinone and oleanane scaffolds. *Med. Chem. Res.* **2012**, *21*, 3568–3580. [[CrossRef](#)]
11. Pingaew, R.; Prachayasittikul, S.; Ruchirawat, S.; Prachayasittikul, V. Synthesis and structure–activity relationship of mono-indole-, bis-indole-, and tris-indole-based sulfonamides as potential anticancer agents. *Mol. Divers.* **2013**, *17*, 595–604. [[CrossRef](#)] [[PubMed](#)]
12. Lai, C.J.; Bao, C.J.; Tao, X.; Wang, J.; Atoyian, R.; Qu, H.; Wang, D.G.; Yin, L.; Samson, M.; Forrester, J.; et al. CUDC-101, a multitargeted inhibitor of histone deacetylase, epidermal growth factor receptor, and human epidermal growth factor receptor 2, exerts potent anticancer activity. *Cancer Res.* **2010**, *70*, 3647–3656. [[CrossRef](#)] [[PubMed](#)]
13. Al-Quawasmeh, R.A.; Huesca, M.; Nedunuri, V.; Peralta, R.; Wright, J.; Lee, Y.; Young, A. Potent antimicrobial activity of 3-(4, 5-diaryl-1H-imidazol-2-yl)-1H-indole derivatives against methicillin-resistant *Staphylococcus aureus*. *Bioorg. Med. Chem. Lett.* **2010**, *20*, 3518–3520. [[CrossRef](#)]
14. Mascal, M.; Modes, K.V.; Durmus, A. Concise photochemical synthesis of the antimalarial indole alkaloid decursivine. *Angew. Chem. Int. Ed. Engl.* **2011**, *50*, 4445–4446. [[CrossRef](#)] [[PubMed](#)]
15. Sechi, M.; Derudas, M.; Dallochio, R.; Dessi, A.; Bacchi, A.; Sannia, L.; Carta, F.; Palomba, M.; Ragab, O.; Chan, C.; et al. Design and synthesis of novel indole β -diketo acid derivatives as HIV-1 integrase inhibitors. *J. Med. Chem.* **2014**, *47*, 5298–5310. [[CrossRef](#)] [[PubMed](#)]
16. Mandour, A.H.; El-Sawy, E.R.; Shaker, K.H.; Mustafa, M.A. Synthesis, anti-inflammatory, analgesic and anticonvulsant activities of 1, 8-dihydro-1-aryl-8-alkyl pyrazolo (3, 4-b) indoles. *Acta Pharm.* **2010**, *60*, 73–88. [[CrossRef](#)] [[PubMed](#)]
17. Narayana, B.; Ashalatha, B.V.; Vijayaraj, K.K.; Fernandes, J.; Sarojini, B.K. Synthesis of some new biologically active 1, 3, 4-oxadiazolyl nitroindoles and a modified Fischer indole synthesis of ethyl nitro indole-2-carboxylates. *Bioorg. Med. Chem.* **2005**, *13*, 4638–4644. [[CrossRef](#)]
18. Ty, N.; Dupeyre, G.; Chabot, G.G.; Seguin, J.; Tillequin, F.; Scherman, D.; Michel, S.; Cachet, X. Synthesis and biological evaluation of new disubstituted analogues of 6-methoxy-3-(3', 4', 5'-trimethoxybenzoyl)-1H-indole (BPR0L075), as potential antivascular agents. *Bioorg. Med. Chem.* **2008**, *16*, 7494–7503. [[CrossRef](#)]
19. Islam, M.S.; Barakat, A.; Al-Majid, A.M.; Ali, M.; Yousuf, S.; Choudhary, M.I.; Khalil, R.; Ul-Haq, Z. Catalytic asymmetric synthesis of indole derivatives as novel α -glucosidase inhibitors in vitro. *Bioorg. Chem.* **2018**, *79*, 350–354. [[CrossRef](#)]
20. Bi, W.; Bi, Y.; Xue, P.; Zhang, Y.; Gao, X.; Wang, Z.; Li, M.; Baudy-Floc'h, M.; Ngerebara, N.; Gibson, K.M.; et al. Synthesis and characterization of novel indole derivatives reveal improved therapeutic agents for treatment of ischemia/reperfusion (I/R) injury. *J. Med. Chem.* **2010**, *53*, 6763–6767. [[CrossRef](#)]
21. Boraie, A.T.; Ghabbour, H.A.; Gomaa, M.S.; El Ashry, E.S.H.; Barakat, A. Synthesis and anti-proliferative assessment of triazolo-thiadiazepine and triazolo-thiadiazine scaffolds. *Molecules* **2019**, *24*, 4471. [[CrossRef](#)] [[PubMed](#)]
22. Boraie, A.T.A.; Gomaa, M.S.; El Sayed, E.S.H.; Duerkop, A. Design, selective alkylation and X-ray crystal structure determination of dihydro-indolyl-1,2,4-triazole-3-thione and its 3-benzylsulfanyl analogue as potent anticancer agents. *Eur. J. Med. Chem.* **2017**, *125*, 360–371. [[CrossRef](#)] [[PubMed](#)]
23. Boraie, A.T.; Ashour, H.K.; El Sayed, H.; Abdelmoaty, N.; El-Falouji, A.I.; Gomaa, M.S. Design and synthesis of new phthalazine-based derivatives as potential EGFR inhibitors for the treatment of hepatocellular carcinoma. *Bioorg. Chem.* **2019**, *85*, 293–307. [[CrossRef](#)] [[PubMed](#)]
24. Boraie, A.T.; Singh, P.K.; Sechi, M.; Satta, S. Discovery of novel functionalized 1, 2, 4-triazoles as PARP-1 inhibitors in breast cancer: Design, synthesis and antitumor activity evaluation. *Eur. J. Med. Chem.* **2019**, *182*, 111621. [[CrossRef](#)]
25. Kaur, R.; Dwivedi, A.R.; Kumar, B.; Kumar, V. Recent developments on 1, 2, 4-triazole nucleus in anticancer compounds: A review. *Anti-Cancer Agent. Med. Chem.* **2016**, *16*, 465–489. [[CrossRef](#)]
26. Ayati, A.; Emami, S.; Foroumadi, A. The importance of triazole scaffold in the development of anticonvulsant agents. *Eur. J. Med. Chem.* **2016**, *109*, 380–392. [[CrossRef](#)]

27. Keri, R.S.; Patil, S.A.; Budagumpi, S.; Nagaraja, B.M. Triazole: A Promising Antitubercular Agent. *Chem. Biol. Drug Des.* **2015**, *86*, 410–423. [[CrossRef](#)]
28. Kucukguzel, S.G.; Cikla-Suzgun, P. Recent advances bioactive 1, 2, 4-triazole-3-thiones. *Eur. J. Med. Chem.* **2015**, *97*, 830–870. [[CrossRef](#)]
29. Guo, L.; Wu, M.; Leng, S.; Qiang, Y.; Zheng, X. Synergistic effect of purpald with tartaric acid on the corrosion inhibition of mild steel: From electrochemical to theoretical insights. *Prot. Met. Phys. Chem. Surf.* **2018**, *54*, 917–925. [[CrossRef](#)]
30. Yan, D.; Xiang, Y.; Li, K.; Chen, Y.; Yang, Z.; Guo, D. Synthesis, characterization and properties of 1, 2, 4-triazolo [3-b][1,3,4]thiadiazole derivatives and their europium complexes. *J. Mol. Struct.* **2014**, *1074*, 487–495. [[CrossRef](#)]
31. Hamdy, R.; Ziedan, N.; Ali, S.; El-Sadek, M.; Lashin, E.; Brancale, A.; Jones, A.T.; Westwell, A.D. Synthesis and evaluation of 3-(benzylthio)-5-(1*H*-indol-3-yl)-1,2,4-triazol-4-amines as Bcl-2 inhibitory anticancer agents. *Bioorg. Med. Chem. Lett.* **2013**, *23*, 2391–2394. [[CrossRef](#)] [[PubMed](#)]
32. Altowyan, M.S.; Haukka, M.; Soliman, S.M.; Barakat, A.; Boraei, A.T.A.; Aboelmagd, A. Stereoselective Synthesis of New 4-Aryl-5-indolyl-1,2,4-triazole *S*- and *N*- β -Galactosides: Characterizations, X-ray Crystal Structure and Hirshfeld Surface Analysis. *Crystals* **2023**, *13*, 797. [[CrossRef](#)]
33. Rikagu Oxford Diffraction. *CrysAlisPro*; Rikagu Oxford Diffraction Inc.: Yarnton, UK, 2020.
34. Sheldrick, G.M. Shelxt-integrated space-group and crystal-structure determination. *Acta Cryst.* **2015**, *A71*, 3–8. [[CrossRef](#)] [[PubMed](#)]
35. Sheldrick, G.M. Crystal structure refinement with SHELXL. *Acta Cryst.* **2015**, *C71*, 3–8.
36. Hübschle, C.B.; Sheldrick, G.M.; Dittrich, B. ShelXle: A Qt graphical user interface for SHELXL. *J. Appl. Crystallogr.* **2011**, *44*, 1281–1284. [[CrossRef](#)]
37. Turner, M.J.; McKinnon, J.J.; Wolff, S.K.; Grimwood, D.J.; Spackman, P.R.; Jayatilaka, D.; Spackman, M.A. Crystal Explorer17. University of Western Australia. 2017. Available online: <https://crystalexplorer.net/> (accessed on 30 July 2020).

Disclaimer/Publisher's Note: The statements, opinions and data contained in all publications are solely those of the individual author(s) and contributor(s) and not of MDPI and/or the editor(s). MDPI and/or the editor(s) disclaim responsibility for any injury to people or property resulting from any ideas, methods, instructions or products referred to in the content.